DEFORMATION LOCALISATION IN VISCOELASTIC LIQUID CRYSTAL ELASTOMERS

Rabin Poudel[1*], Yasemin Şengül[1], L. Angela Mihai[1]

[1] School of Mathematics, Cardiff University, Senghennydd Road, Cardiff, CF24 4AG, UK.
PoudelR@cardiff.ac.uk
SengulTezelY@cardiff.ac.uk, MihaiLA@cardiff.ac.uk

Abstract. We develop an effective numerical model for viscoelastic liquid crystal elastomers where contributions due to the polymeric network and the liquid crystal mesogens are clearly defined and represented computationally. Finite element simulations of deformation localisation characteristic to these materials illustrate the efficiency of our approach.

Key words: *liquid crystals elastomers; viscoelasticity; finite element method; mathematical modelling*

1 Introduction

Combining the self-organisation of liquid crystals (LCs) with the flexibility of elastomers results in a special class of stimuli-responsive solid materials called liquid crystal elastomers (LCEs). These materials deform in response to changes in the LC orientation driven by temperature variation, electric, magnetic, or optical fields, and their LC alignment changes when mechanical loads are applied. Their unique properties make LCEs a top choice for bioinspired devices and engineering designs. Experimental evidence further suggests that, under certain conditions, the stress-strain curves of nematic LCEs display strain-rate dependent hysteresis during loading and unloading [5], but the modelling of this phenomenon remains an open question [6]. In this study, we devise a mathematical model for viscoelastic LCEs where different contributions are clearly defined and simulated computationally. To develop efficient numerical models for nonlinear viscoelastic deformations of LCEs, the finite element method (FEM) is employed. This is well-suited for capturing complex behaviours and interactions, providing detailed insights into complex mechanical responses under various boundary conditions and internal constraints.

2 Kinematics and model function

The elastic behaviour of a nematic LCE can be described by a strained-energy density function of the form [1]

$$\mathbb{W} = \mathbb{W}^{(1)}(\boldsymbol{F}) + \mathbb{W}^{(2)}(\boldsymbol{A}) + \mathbb{W}^{(3)}(\mathbf{Grad}\ \boldsymbol{n}), \tag{1}$$

where $\boldsymbol{F}$ is the deformation gradient from the cross-linking state, $\boldsymbol{A} = \boldsymbol{G}^{-1}\boldsymbol{F}\boldsymbol{G}_0$ is the local elastic deformation tensor, and $\boldsymbol{G}_0$ and $\boldsymbol{G}$ are the natural deformation tensors in reference and current configuration, respectively (see Fig. 1a). Assuming that the LCE is intrinsically uniaxial, these tensors take the form

$$\boldsymbol{G}_0 = a_0^{-1/6}\boldsymbol{I} + \left(a_0^{1/3} - a_0^{-1/6}\right)\boldsymbol{n}_0 \otimes \boldsymbol{n}_0, \qquad \boldsymbol{G} = a^{-1/6}\boldsymbol{I} + \left(a^{1/3} - a^{-1/6}\right)\boldsymbol{n} \otimes \boldsymbol{n}, \tag{2}$$

where $\boldsymbol{n}_0$ and $\boldsymbol{n}$ represent the local nematic director, while a_0 and a denote the natural shape parameter in the reference and current configuration, respectively, and $\boldsymbol{I}$ is the tensor identity.

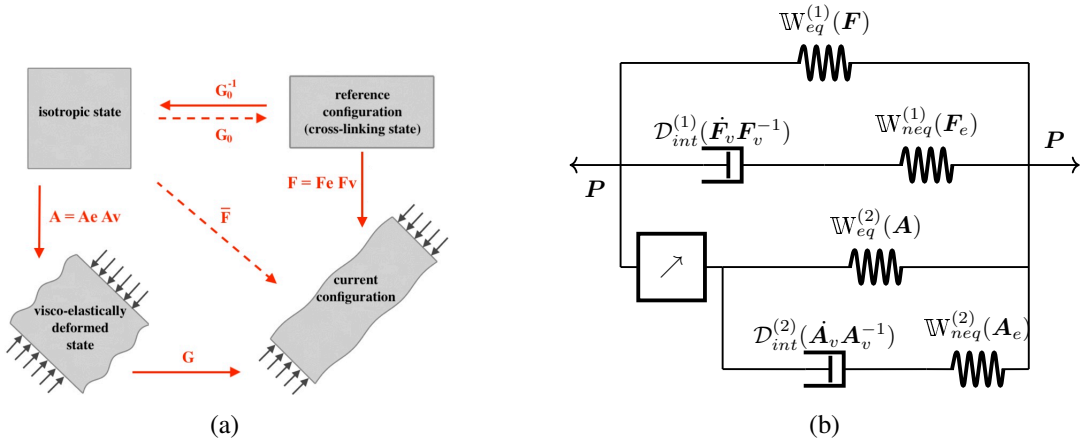

Figure 1: (a) Multiplicative decomposition of the deformation gradient and (b) Rheology model for the viscoelastic behaviour of a nematic LCE.

To model the viscoelastic properties of the LCE, one popular approach used for the rubber network [2] is to decompose the deformation gradient into an elastic and a viscous part. Here, we extend this approach to both the tensors $\boldsymbol{F}$ and $\boldsymbol{A}$, which we decompose multiplicatively as (see Fig. 1b)

$$\boldsymbol{F} = \boldsymbol{F}_e\boldsymbol{F}_v, \qquad \boldsymbol{A} = \boldsymbol{A}_e\boldsymbol{A}_v. \tag{3}$$

The model function given by (1) is then recast as

$$\mathbb{W} = \mathbb{W}^{(1)}_{eq}(\boldsymbol{F}) + \mathbb{W}^{(1)}_{neq}(\boldsymbol{F}_v) + \mathbb{W}^{(2)}_{eq}(\boldsymbol{A}) + \mathbb{W}^{(2)}_{neq}(\boldsymbol{A}_v) + \mathbb{W}^{(3)}(\mathbf{Grad}\,\boldsymbol{n}), \tag{4}$$

where the equilibrium terms with an '*eq*' index describe the rate-independent elastic response and the non-equilibrium terms with a '*neq*' index characterise the rate-dependent viscous response of the material. For simplicity, we choose

$$\mathbb{W}^{(1)}_{eq}(\boldsymbol{F}) = \frac{\mu^{(1)}_{eq}}{2}\left[\mathrm{tr}\,(\boldsymbol{F}^T\boldsymbol{F}) - 3\right], \qquad \mathbb{W}^{(1)}_{neq}(\boldsymbol{F}) = \frac{\mu^{(1)}_{neq}}{2}\left[\mathrm{tr}\,(\boldsymbol{F}_e^T\boldsymbol{F}_e) - 3\right], \tag{5}$$

$$\mathbb{W}^{(2)}_{eq}(\boldsymbol{F}) = \frac{\mu^{(1)}_{eq}}{2}\left[\mathrm{tr}\,(\boldsymbol{A}^T\boldsymbol{A}) - 3\right], \qquad \mathbb{W}^{(2)}_{neq}(\boldsymbol{F}) = \frac{\mu^{(1)}_{neq}}{2}\left[\mathrm{tr}\,(\boldsymbol{A}_e^T\boldsymbol{A}_e) - 3\right], \tag{6}$$

i.e., neo-Hookean-type models for the components of $\mathbb{W}^{(1)}$ and neo-classical-type models [3] for the components of $\mathbb{W}^{(2)}$. These can be replaced with more sophisticated models if necessary. We also set $\mathbb{W}^{(3)}(\mathbf{Grad}\,\boldsymbol{n}) = \frac{\mathrm{k}}{2}|\mathbf{Grad}\,\boldsymbol{n}|^2$, which is the one-term Frank energy density [3].

3 Thermodynamics consistency and evolution equations

Assuming an in-plane nematic orientation $\boldsymbol{n} = (\cos\theta, \sin\theta, 0)$, the second law of thermodynamics gives the isothermal Clausius-Duhem inequality requirement

$$\mathcal{D}_{int} = \boldsymbol{P} : \dot{\boldsymbol{F}} - \dot{\mathbb{W}} + g_\theta\dot{\theta} + \boldsymbol{\pi}_\theta \cdot (\mathrm{Grad}\,\theta)^{\cdot} \geq 0, \tag{7}$$

where $\mathcal{D}_{int}$ is the internal dissipation rate, $\boldsymbol{P}$ is the first Piola-Kirchhoff stress tensor, g_θ and $\boldsymbol{\pi}_\theta$ are the orientational stresses., and the over-dot represents differentiation with respect to time in Newton notation. Following the Coleman-Noll procedure [4], we have

$$\boldsymbol{P} = \frac{\partial \mathbb{W}}{\partial \boldsymbol{F}} + \frac{\partial \mathbb{W}}{\partial \boldsymbol{A}}, \qquad g_\theta = \frac{\partial \mathbb{W}}{\partial \theta}, \qquad \boldsymbol{\pi}_\theta = \frac{\partial \mathbb{W}}{\partial \mathrm{Grad}\,\theta}, \tag{8}$$

and the inequality (7) reduces to

$$\mathcal{D}_{int} = -\frac{\partial \mathbb{W}}{\partial \boldsymbol{F}_v} : \dot{\boldsymbol{F}}_v - \frac{\partial \mathbb{W}}{\partial \boldsymbol{A}_v} : \dot{\boldsymbol{A}}_v \geq 0. \tag{9}$$

To satisfy this inequality, we choose

$$\mathcal{D}_{int} = \frac{\eta^{(1)}}{2} \dot{\boldsymbol{F}}_v \boldsymbol{F}_v^{-1} : \dot{\boldsymbol{F}}_v \boldsymbol{F}_v^{-1} + \frac{\eta^{(2)}}{2} \dot{\boldsymbol{A}}_v \boldsymbol{A}_v^{-1} : \dot{\boldsymbol{A}}_v \boldsymbol{A}_v^{-1}, \tag{10}$$

where $\eta^{(1)}$ and $\eta^{(2)}$ are the viscous parameters. By comparing the above expression with the inequality (9), we obtain

$$\frac{\partial \mathbb{W}}{\partial \boldsymbol{F}_v} = -\frac{\eta^{(1)}}{2} \dot{\boldsymbol{F}}_v \boldsymbol{F}_v^{-1} \boldsymbol{F}_v^{-T}, \qquad \frac{\partial \mathbb{W}}{\partial \boldsymbol{A}_v} = -\frac{\eta^{(2)}}{2} \dot{\boldsymbol{A}}_v \boldsymbol{A}_v^{-1} \boldsymbol{A}_v^{-T}, \tag{11}$$

as the evolution equations for $\boldsymbol{F}_v$ and $\boldsymbol{A}_v$, respectively.

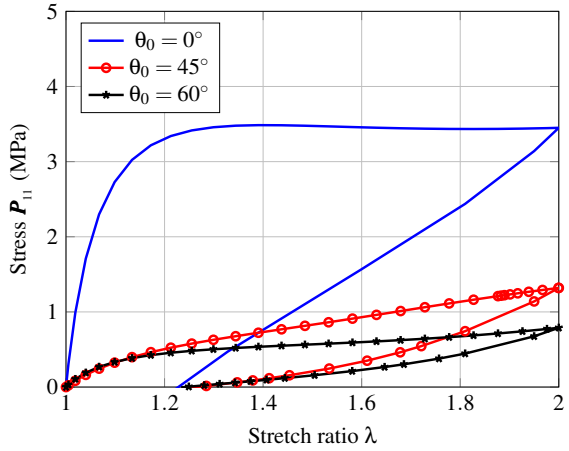

(a) Influence of initial director angle with constant strain rate of $\dot{\lambda} = 0.1\,s^{-1}$.

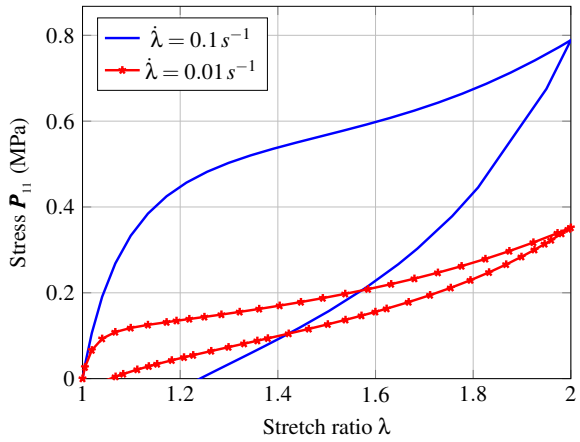

(b) Influence of strain rate $\dot{\lambda}$ with the initial director angle of $\theta_0 = 60°$.

Figure 2: Loading and unloading stress-strain relationship in uniaxial extension.

4 Numerical results

We implemented the theoretical model described above within the finite element software FEBio [7]. In our numerical examples, we took a sample of LCE with length 15 mm, width 3 mm and thickness

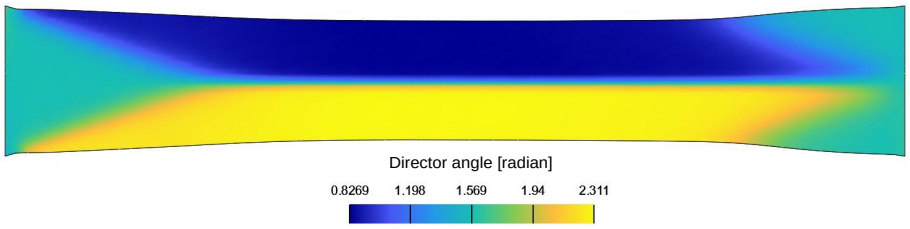

Figure 3: Shear striping developed in the LCE sample with vertical initial director ($\theta_0 = 90^\circ$) when stretched horizontally at strain $\lambda - 1 = 0.2$ and strain rate $\dot{\lambda} = 0.001\, s^{-1}$.

0.1 mm. The material parameter used are $\mu_{eq}^{(1)} = 0.1$ MPa, $\mu_{neq}^{(1)} = 1.0$ MPa, $\mu_{eq}^{(2)} = 1.0$ MPa , $\mu_{neq}^{(2)} = 20$ MPa, $\eta^{(1)} = 20$ MPa·s, $\eta^{(2)} = 100$ MPa·s, $a_0 = a = 5.5$ and $\mathtt{k} = 10^{-11}$ N. The sample was loaded in the longitudinal direction with clamped boundary conditions at the ends. First, we studied the influence of the initial director angle θ_0 on the stress-strain relationship imposed with constant strain rate of 0.1 s^{-1} (see Fig. 2a). Second, we looked at the effects of different strain rates on the sample with $\theta_0 = 60^o$ (see Fig. 2b). Our model function shows stress-train relationships that are qualitatively similar to those obtained experimentally and the model parameters can be calibrated to measurements for further quantitative estimations. We also applied the numerical model to capture shear striping in stretched LCEs (see Fig. 3). This is an important mechanical behaviour which distinguishes LCEs from other rubber-like and soft materials.

5 Conclusions

We captured the nonlinear deformations of nematic LCEs by combining, for the first time, the viscoelasticity of the polymeric network with the rotation of the nematic director. Numerical examples of deformation localisation which are specific to LCEs demonstrate the efficiency of our approach.

REFERENCES

[1] Poudel, R., Şengül, Y. and Mihai, L.A. 2024. Deformation localisation in stretched liquid crystal elastomers, *Mechanics of Soft Materials*, 6, 8 (doi: 10.1007/s42558-024-00063-2).

[2] Reese, S. and Govindjee, S. A theory of finite viscoelasticity and numerical aspects. *International Journal Of Solids And Structures*. **35**, 3455-3482 (1998,9).

[3] Warner, M. and Terentjev, E. *Liquid Crystal Elastomers*. (Oxford University Press, USA,2007).

[4] Coleman, B. and Noll, W. The thermodynamics of elastic materials with heat conduction and viscosity. *Archive For Rational Mechanics And Analysis*. **13**, 167-178 (1963,12).

[5] Hotta, A. and Terentjev, E. 2001. Long-time stress relaxation in polyacrylate nematic liquid crystalline elastomers, *Journal of Physics: Condensed Matter*, 13(50), 11453-11464 (doi: 10.1088/0953-8984/13/50/305).

[6] Chehade, A.E.H., Shen, B., Yakacki, A.M., Nguyen, T.D. and Govindjee S. 2024. Finite element modeling of viscoelastic liquid crystal elastomers, *International Journal for Numerical Methods in Engineering* (doi: 10.1002/nme.7510).

[7] Maas, S., Ellis, B., Ateshian, G. and Weiss, J. FEBio: Finite Elements for Biomechanics. *Journal Of Biomechanical Engineering*. **134** (2012,1).